

# Identification of Hypoxic Cells Using an Organotellurium Tag Compatible with Mass Cytometry\*\*

Landon J. Edgar, Ravi N. Vellanki, Adrienne Halupa, David Hedley, Bradly G. Wouters, and Mark Nitz\*

**Abstract:** Mass cytometry (MC) offers unparalleled potential for the development of highly parameterized assays for characterization of single cells within heterogeneous populations. Current reagents compatible with MC analysis employ antibody-metal-chelating polymer conjugates to report on the presence of biomarkers. Here, we expand the utility of MC by developing the first activity-based probe designed specifically for use with the technology. A compact MC-detectable telluroether is linked to a bioreductively sensitive 2-nitroimidazole scaffold, thereby generating a probe sensitive to cellular hypoxia. The probe exhibits low toxicity and is able to selectively label  $O_2$ -deprived cells. A proof-of-concept experiment employing metal-bound DNA intercalators demonstrates that a heterogeneous mixture of cells with differential exposure to  $O_2$  can be effectively discriminated by the quantity of tellurium-labeling. The organotellurium reagents described herein provide a general approach to the development of a large toolkit of MC-compatible probes for activity-based profiling of single cells.

**M**ultiparameter analysis of single cells has traditionally been performed using fluorescence-based flow cytometry (FBFC); a technique that has transformed understanding of cellular heterogeneity. As scientists begin to ask increasingly complex questions about relationships between large numbers of biological parameters, the limitations inherent to FBFC have become apparent. Specifically, the number of fluorophore tags that may be employed simultaneously in any given FBFC experiment is limited by spectral overlap, thereby prohibiting a highly parameterized analysis.<sup>[1]</sup> The introduction of mass cytometry (MC) has provided a means for overcoming this limitation. In place of fluorophores, MC

uses stable isotopes with high atomic mass as tags and harnesses the sensitivity, dynamic range, and single mass unit resolution of inductively coupled plasma mass spectrometry to allow for highly parameterized experiments (theoretically over 100 parameters).<sup>[2–4]</sup> This technology has been successfully used to monitor differential responses across the human hematopoietic continuum based on 34 unique parameters.<sup>[4]</sup> Recent work has adapted MC-compatible reagents for 32-parameter imaging of breast cancer tissue, revealing spatial variations in tumor heterogeneity with an unprecedented level of detail.<sup>[5]</sup>

To fully realize the parameterization of MC requires many reagents bearing unique heavy isotopes ( $\geq 100$  amu) with a low biological background that report on meaningful biological parameters. To date, the most successful reagents developed have been bifunctional polymers that chelate lanthanide ions and allow for antibody conjugation (MaxPar Reagents, Figure 1 a).<sup>[6]</sup> Additionally, metal chelates that bind or may be incorporated into DNA have been exploited (Figure 1 b).<sup>[7]</sup> The success that researchers have had with these reagents cannot be understated; however, the potential of MC should not be limited to reagents that measure static biomarkers. Probes for specific enzyme activities would unlock new dimensions to MC analysis (Figure 1 c). Here,

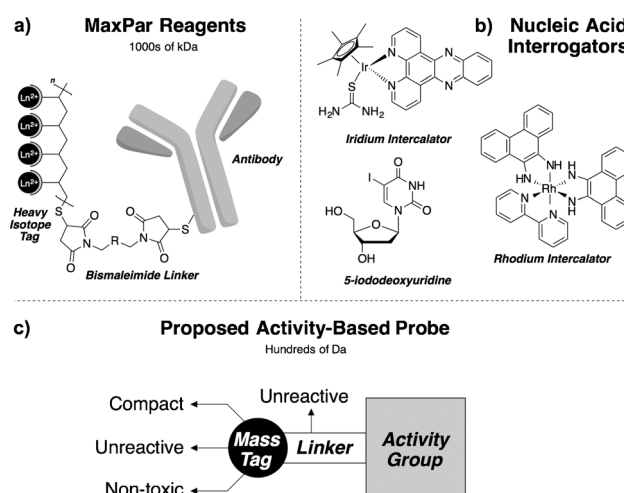


**Figure 1.** a) Generalized structure of commercially available bifunctional lanthanide-chelating polymer-antibody conjugates (MaxPar reagents). b) Structures of the heavy-isotope-containing nucleic acid intercalators employed in this study and the unnatural nucleoside analogue 5-iododeoxyuridine (IdU). c) Requirements and generalized design of a MC-compatible probe for studying dynamic/active biochemical processes.

[\*] L. J. Edgar, Dr. A. Halupa, Prof. M. Nitz  
Department of Chemistry, University of Toronto  
80 St. George Street, Toronto, Ontario, M5S 3H6 (Canada)  
E-mail: mnitz@chem.utoronto.ca

Dr. R. N. Vellanki, Prof. D. Hedley, Prof. B. G. Wouters  
Princess Margaret Cancer Centre, Departments of Radiation  
Oncology and Medical Biophysics, University Health Network  
101 College Street, Toronto, Ontario, M5G 1L7 (Canada)

[\*\*] We acknowledge Tina Chen for collecting cytometry data, the U of T NMR facility for spectral analysis (CFI/ORF no 19119), the AIMS laboratory for mass spectrometric analysis, Dr. R. Williams, Dr. L. Willis, and Dr. Q. Chang for productive discussions and funding from the Natural Science and Engineering Research Council (NSERC), DVS Sciences, and the Canadian Cancer Society (no 702397).

Supporting information for this article is available on the WWW under <http://dx.doi.org/10.1002/anie.201405233>.

we introduce a new approach for the development of activity-based probes compatible with MC technology using a compact telluroether scaffold.

Tellurium provides favorable characteristics for the development of small MC probes. The element forms telluroether and tellurophene functionalities which are small and lipophilic; properties which we hypothesize will minimize perturbation of attached biologically sensitive functionalities (i.e. activity-based groups), thus preserving their biological activity. This is in direct contrast to the lanthanide-chelating polymers used as mass tags in MaxPar reagents, because these groups are large and polar (Figure 1 a). Additionally, five stable tellurium isotopes are available commercially, thereby allowing for multiple MC-distinguishable probes to be generated using identical chemistry. As a proof of concept of such a probe, we have targeted cellular hypoxia due to its importance in tumor biology and the well-defined chemical methods for interrogation.

The development of hypoxic regions is a common characteristic of most solid tumors and is associated with radiation and chemotherapy resistance, as well as increased metastasis.<sup>[8]</sup> Levels of hypoxia also vary widely amongst patients, and are strongly associated with poor clinical outcome in several tumor types. Within individual tumors, hypoxia is spatially heterogeneous and often characterized by gradients of oxygenation extending from normal levels near the vasculature to near anoxia at the borders with necrosis.<sup>[9]</sup> Importantly, oxygen levels in some tumor regions also fluctuate over time due to transient changes in vessel perfusion. Areas of fluctuating hypoxia may be particularly important in driving poor prognosis, but at present are difficult to quantitate in patients.<sup>[10]</sup> Current understanding of tumor hypoxia has been greatly facilitated by the availability of chemical probes constructed around a 2-nitroimidazole (2-NI) functionality such as pimonidazole (Pimo) and EF-5.<sup>[11]</sup> These probes are reduced by one electron reductases, such as PORs (p450 oxidoreductase), which act on a variety of nitroaryl compounds (Scheme 1 b).<sup>[14]</sup> Studies suggest that upon reduction of the 2-NI to a 2-(hydroxy amino)imidazole (**5**), hydroxide is liberated and an electrophilic 2-(nitrenium)imidazole ion (**6**) is generated, which reacts irreversibly with free thiols in the

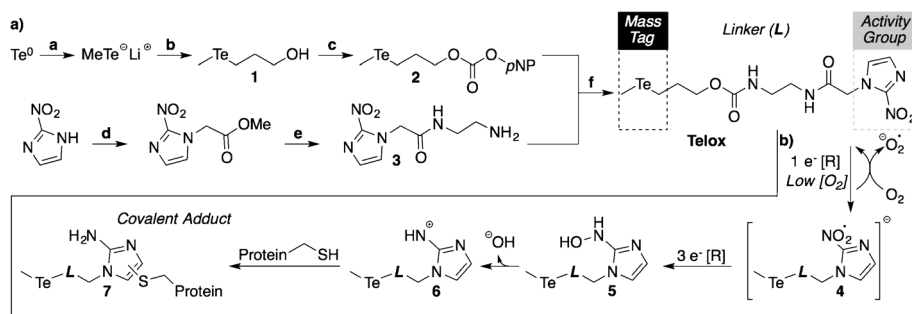
hypoxic environment. This produces protein-2-(amino)imidazole adducts (**7**) effectively “tagging” the cell. Generation of the initial nitro radical (**4**) is a rapidly reversible process in the presence of molecular oxygen and thus generation of the active nitrenium labeling agent is slow under normoxic conditions. In the case of Pimo and EF-5, the detection is mediated by immunostaining, although similar 2-NI compounds have been developed which incorporate <sup>18</sup>F to allow for detection through positron emission tomography.<sup>[12]</sup> Recently, hypoxia probes based on 2-NIs have been developed that implement alternative imaging modalities such as single-photon emission computed tomography, magnetic resonance imaging, or near-infrared fluorescence.<sup>[13]</sup>

To adapt the 2-NI functionality for MC detection we identified an organotellurium scaffold that was compact, amenable to high yielding synthesis, stable under physiological conditions, and relatively nontoxic. Reports of organotellurium toxicity have focused mainly on aryltelluroethers; however, the limited reports available suggest the more compact dialkyl telluroethers are less toxic.<sup>[15–17]</sup> Focusing on telluroethers, we opted to use a compact unsymmetric methyl alkyl telluride functionality (**1**, Scheme 1 a) with a reactive hydroxy handle for further chemical manipulation. This group was accessed through treatment of elemental tellurium with methyllithium, followed by alkylation of the resultant nucleophilic methyltelluride salt by 3-chloropropan-1-ol (Scheme 1 a).<sup>[18]</sup> The resultant telluroether alcohol (**1**) was then treated with *p*-nitrophenyl chloroformate to afford the carbamylating reagent **2**. The primary amine-bearing 2-NI scaffold (**3**) was then easily carbamylated to afford the final hypoxia probe, designated “Telox” (Scheme 1 a). This compound is stable for months if stored in the dark as a solid and under an inert atmosphere at –20 °C. At ambient light and oxygen levels the probe has a *t*<sub>1/2</sub> > 48 h in solution (see the Supporting Information). Due to a downfield shift of the Te-CH<sub>3</sub> resonance in the <sup>1</sup>H NMR spectrum of the probe after prolonged exposure to ambient atmosphere, we hypothesize that the major degradation product upon exposure to atmospheric oxygen is the telluroxide species or a hydrate thereof.

The proliferative toxicity of Telox was measured in

HCT116 cells by confluency analysis (Figure S1). This experiment suggested that proliferation was only mildly affected up to the maximum probe concentration evaluated (400 μM) under both normoxic (21 % O<sub>2</sub>) and hypoxic (0.2 % O<sub>2</sub>) conditions. An orthogonal assay was performed using the reduction of WST-1 as a metric for metabolic toxicity induced by the presence of Telox. In Jurkat cells, this experiment indicated a metabolic IC<sub>50</sub> of 200 ± 20 μM (Figure S2).

As a surrogate for a POR enzyme, the sensitivity of Telox to enzyme-mediated reduction was



**Scheme 1.** a) a: MeLi (≈ 1 equiv), THF, 22 °C, 10 min; b: 3-chloro-1-propanol (1.0 equiv), THF, –192 °C, 2 h, 72%; c: *p*-nitrophenyl chloroformate (1.05 equiv), pyridine (2.1 equiv), THF, 22 °C, 2 h, 75%; d: methylbromoacetate (1.0 equiv), K<sub>2</sub>CO<sub>3</sub> (1.5 equiv), tetrabutylammonium iodide (0.022 equiv), MeCN, reflux, 3 h, 60%; e: ethylenediamine (4.0 equiv), MeOH, 22 °C, 18 h, quant.; f: pyridine (3.0 equiv), MeOH, 22 °C, 2 h, 70%. b) Enzyme-catalyzed reduction of the 2-nitroimidazole functionality to produce the electrophilic protein-labeling nitrenium ion **6**.

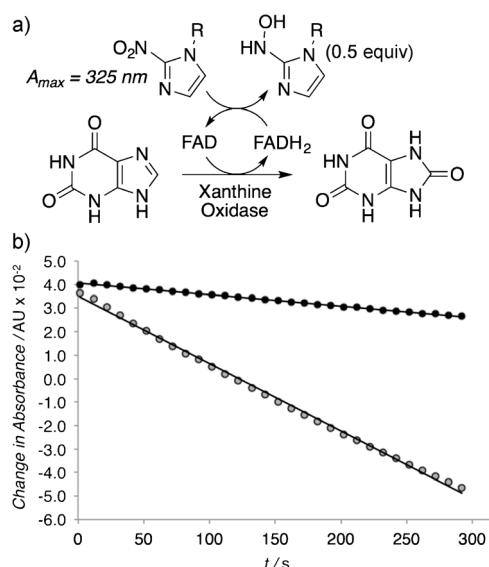


**Figure 2.** a) Xanthine oxidase catalyzed reduction of a generalized 2-nitroimidazole using xanthine as a source of electrons and FAD as a cofactor. b) Change in UV absorption over time at 325 nm for the anaerobic enzymatic reduction of the 2-nitroimidazole component of Pimonidazole (black circles) or Telox (grey circles). [2-NI] = 100  $\mu$ M, [xanthine] = 500  $\mu$ M, 0.2 units XO.

evaluated using bovine xanthine oxidase (XO; Figure 2a).<sup>[19]</sup> Following the loss of the 2-nitroimidazole absorption at 325 nm during XO-mediated oxidation of xanthine to uric acid demonstrated that under normoxia no reduction of Telox was observed (data not shown); however, under hypoxic conditions a clear loss of the 2-nitroimidazole occurred (Figure 2b). Interestingly the rate of reduction was higher for Telox than that for Pimo, one of the most commonly used hypoxia probes. These experiments suggest that the reduction potential and structure of Telox are compatible with enzyme-mediated reduction. Additionally, the telluroether functionality does not appear to have an inhibitory effect on the metal-containing active site of XO under these conditions.

Having confirmed that Telox could be enzymatically reduced in vitro, we evaluated the ability of the probe to label HCT116 cells under normoxic and hypoxic conditions (Figure 3). In an atmosphere that contained <0.02 %  $O_2$ , robust labeling ( $\approx 3.4$ -fold) was detected by ICP-MS analysis of whole cell pellets when cells were incubated for 3 h in media containing Telox (100  $\mu$ M). A substantially lower tellurium concentration was detected under all other concentrations of  $O_2$ , indicating that the labeling ability of Telox is indeed oxygen-dependent. This level of oxygen sensitivity is similar to that observed with EF5, which displays dramatic increases in labeling only below 0.1 %  $O_2$ .<sup>[20]</sup> Given the similar oxygen sensitivity, Telox should be useful as a MC-compatible surrogate for the widely used probes EF5 or Pimo.

Next, we investigated the ability of Telox to identify hypoxic cells in a mixture using MC. HCT116 cells were incubated under normoxic or anoxic conditions in the presence of Telox as detailed above. Following exposure to Telox the cells were washed and fixed. To correlate the cellular tellurium content with oxygen exposure, we used

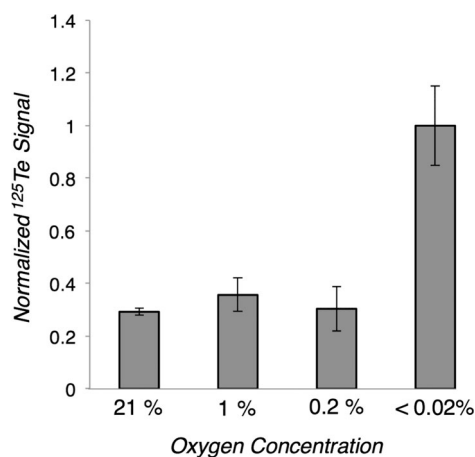


**Figure 3.** Traditional ICP-MS analysis of the tellurium content of whole HCT116 cell pellets as a function of cellular oxygen exposure. [Telox] = 100  $\mu$ M, incubation time = 3 h.

metal-containing nucleic acid intercalators as internal standards for oxygen exposure. Cells incubated under normoxic conditions were treated with a rhodium-containing nucleic acid intercalator (Figure 1b), whereas cells incubated under anoxic conditions were treated with an iridium-containing nucleic acid intercalator (Figure 1b).<sup>[7]</sup> Both samples were washed separately, combined, and injected onto a second-generation CyTOF instrument for MC analysis (Figure 4a). Generation of a density plot of event length versus  $^{130}\text{Te}$  signal clearly indicated the presence of two distinct populations of cells (Figure 4b). Gating each population [high  $^{130}\text{Te}$  (median  $\approx 120$  cts) or low  $^{130}\text{Te}$  (median  $\approx 30$  cts)] and outputting  $^{193}\text{Ir}$  versus  $^{103}\text{Rh}$  density plots from these gates indicated that cells which contained a high relative amount of  $^{130}\text{Te}$  possessed a very high  $^{193}\text{Ir}$  content and a low  $^{103}\text{Rh}$  content (Figure 4c). Conversely, cells that produced a lower  $^{130}\text{Te}$  signal contained far less  $^{193}\text{Ir}$  and a comparatively large amount of  $^{103}\text{Rh}$  (Figure 4d). These results are consistent with expectations, as MC analysis was able to deconvolute the two cell populations to a high degree of resolution using tellurium content as a metric for the oxygen concentration to which cells were exposed. The non-zero  $^{193}\text{Ir}$  signal observed in cells incubated under normoxic conditions was likely due to leeching of less tightly bound Ir intercalator between cell populations after mixing. This is supported by the observation that cells exposed only to the Rh intercalator and not mixed with Ir-stained cells exhibit a near-zero  $^{193}\text{Ir}$  signal (Figure S3).

Finally, in an attempt to further confirm the mode of action, we evaluated the ability of Telox to compete for the same bioreductive pathway as the known hypoxia probe Pimo. Incubation of HCT116 cells in media that contained both probes at equal concentrations (100  $\mu$ M) reduced the tellurium labeling by 1.7-fold when compared to the signal in the absence of Pimo as indicated by CyTOF analysis (Figure 4e). This result suggests that these probes compete for at least some of the same reductase enzymes and that Telox should be a reliable surrogate for Pimo when studying cellular hypoxia.

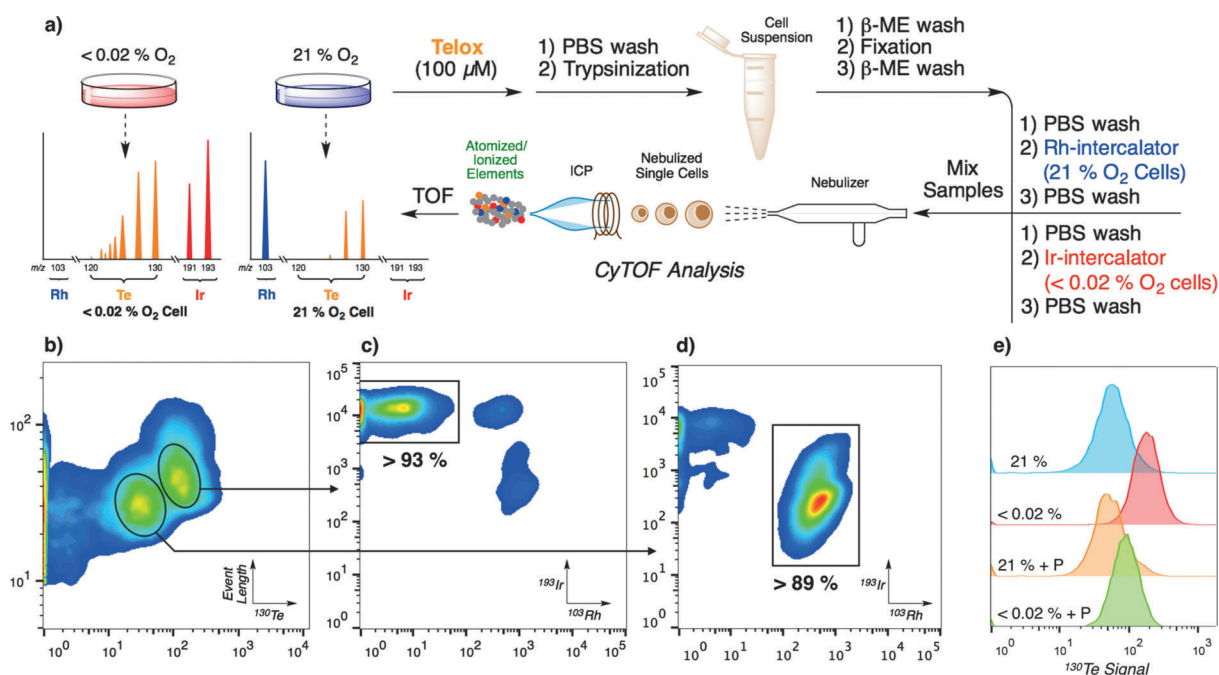


**Figure 4.** a) Schematic representation of Telox cell labeling for analysis by mass cytometry on a second-generation CyTOF instrument. b) Density map of signal event length vs. <sup>130</sup>Te signal (arbitrary units). c) Density plot output from the top-right gate in (b) of the <sup>193</sup>Ir signal versus the <sup>103</sup>Rh signal. More than 93 % of the detected events fall in the square gate. d) Density plot output from the bottom-left gate in (b) of the <sup>193</sup>Ir signal versus the <sup>103</sup>Rh signal. More than 89 % of the detected events fall in the square gate. e) Population histograms of cell <sup>130</sup>Te content. Oxygen concentrations are listed as numerical percentages, P = Pimonidazole (100 μM). Blue and red histograms are Pimonidazole-negative controls. Orange and green histograms are the Pimonidazole-positive competition experiments. Note: warmer colors in density plots indicate higher cell population density.

Moving forward, we propose that the MC-compatible hypoxia probe developed in this report will be of value for the study of complex relationships between hypoxia and tumor biochemistry through the development of highly parameter assays in combination with MaxPar reagents. Furthermore, experiments can be envisioned in which isotopically pure tellurium probes are synthesized and employed in pulse-chase-type experiments to identify the effects that various xenobiotic agents have on the hypoxic response. Our probe is superior to fluorophore-based molecules for this purpose because isotopologs of Telox would be structurally identical and thus have identical pharmacokinetics/dynamics, unlike 2-NIs conjugated to structurally diverse fluorophores. Additionally, the tellurium-containing *p*-nitrophenyl carbonate ester **2** is a versatile reagent for carbamylation of amines, thus presenting a general methodology for accessing new tellurium-containing activity-based probes to be used with MC.

Received: May 13, 2014

Revised: July 9, 2014

Published online: September 3, 2014

**Keywords:** activity-based probes · mass cytometry · multiparameter analysis · organotellurium compounds · tumor hypoxia

[1] S. C. Bendall, G. P. Nolan, M. Roederer, P. K. Chattopadhyay, *Trends Immunol.* **2012**, *33*, 323.

- [2] O. Ornatsky, D. Bandura, V. Baranov, M. Nitz, M. A. Winnik, S. Tanner, *J. Immunol. Methods* **2010**, *361*, 1.
- [3] O. Ornatsky, R. Kinach, D. R. Bandura, X. Lou, S. D. Tanner, V. I. Baranov, M. Nitz, M. A. Winnik, *J. Anal. At. Spectrom.* **2008**, *23*, 463.
- [4] S. C. Bendall, E. F. Simonds, P. Qiu, E. D. Amir, P. O. Krutzik, R. Finck, R. V. Bruggner, R. Melamed, A. Trejo, O. I. Ornatsky, R. S. Balderas, S. K. Plevritis, K. Sachs, D. Pe'er, S. D. Tanner, G. P. Nolan, *Science* **2011**, *332*, 687.
- [5] a) C. Giesen, H. A. O. Wang, D. Schapiro, N. Zivanovic, A. Jacobs, B. Hattendorf, P. J. Schüffler, D. Grolimund, J. M. Buhmann, S. Brandt, Z. Varga, P. J. Wild, D. Günther, B. Bodenmiller, *Nat. Methods* **2014**, *11*, 417; b) M. Angelo, S. C. Bendall, R. Finck, M. B. Hale, C. Hitzman, A. D. Borowsky, R. M. Levenson, J. B. Lowe, S. D. Liu, S. Zhao, Y. Natkunam, G. P. Nolan, *Nat. Med.* **2014**, *20*, 436.
- [6] X. Lou, G. Zhang, I. Herrera, R. Kinach, O. Ornatsky, V. Baranov, M. Nitz, M. A. Winnik, *Angew. Chem. Int. Ed.* **2007**, *46*, 6111; *Angew. Chem.* **2007**, *119*, 6223.
- [7] a) O. I. Ornatsky, X. Lou, M. Nitz, S. Schäfer, W. S. Sheldrick, V. I. Baranov, D. R. Bandura, S. D. Tanner, *Anal. Chem.* **2008**, *80*, 2539; b) G. K. Behbehani, S. C. Bendall, M. R. Clutter, W. J. Fantl, G. P. Nolan, *Cytometry Part A* **2012**, *81*, 552.
- [8] M. W. Dewhirst, Y. Cao, B. Moeller, *Nat. Rev. Cancer* **2008**, *7*, 25.
- [9] M. Nordmark, S. M. Bentzen, V. Rudat, D. Brizel, E. Lartigau, P. Stadler, A. Becker, M. Adam, M. Molls, J. Dunst, D. J. Terris, J. Overgaard, *Radiother. Oncol.* **2005**, *77*, 18.
- [10] J. M. Brown, W. R. Wilson, *Nat. Rev. Cancer* **2004**, *4*, 437.
- [11] a) W. R. Wilson, M. P. Hay, *Nat. Rev. Cancer* **2011**, *11*, 393; b) S. Kizaka-Kondoh, H. Konse-Nagasawa, *Cancer Sci.* **2009**, *11*, 1366; c) M. A. Varia, D. P. Calkins-Adams, L. H. Rinker, A. S. Kennedy, D. B. Novotny, W. C. Fowler Jr., J. A. Raleigh, *Gynecol. Oncol.* **1998**, *71*, 270.



- [12] L. S. Ziemer, S. M. Evans, A. V. Kachur, A. L. Shuman, C. A. Cardi, W. T. Jenkins, J. S. Karp, A. Alavi, W. R. Dolbier, Jr., C. J. Koch, *Eur. J. Nucl. Med.* **2003**, *30*, 259.
- [13] a) F. A. Rojas-Quijano, G. Tircs , E. T. Beny , Z. Baranyai, H. T. Hoang, F. K. K lman, P. K. Gulaka, V. D. Kodibagkar, S. Aime, Z. Kov cs, A. D. Sherry, *Chem. Eur. J.* **2012**, *18*, 9669; b) C. Hsia, F. Huang, G. Hung, L. Shen, C. Chen, H. Wang, *Appl. Radiat. Isot.* **2011**, *69*, 649; c) K. Okuda, Y. Okabe, T. Kadonoso, T. Ueno, B. G. M. Youssif, S. Kizaka-Kondoh, H. Nagasawa, *Bioconjugate Chem.* **2012**, *23*, 324.
- [14] a) R. A. McClelland, R. Panicucci, A. M. Rauth, *J. Am. Chem. Soc.* **1985**, *107*, 1762; b) J. L. Bolton, R. A. McClelland, *J. Am. Chem. Soc.* **1989**, *111*, 8172; c) R. J. Hodgkiss, *Anti-Cancer Drug Des.* **1998**, *13*, 687; d) D. C. Heimbrook, A. C. Sartorelli, *Mol. Pharmacol.* **1985**, *29*, 168.
- [15] L. A. Ba, M. D ring, V. Jamier, C. Jacob, *Org. Biomol. Chem.* **2010**, *8*, 4203.
- [16] L. Engman, N. Al-Maharik, M. McNaughton, A. Birmingham, G. Powis, *Bioorg. Med. Chem.* **2003**, *11*, 5091.
- [17] L. Engman, T. Kanda, A. Gallegos, R. Williams, G. Powis, *Anti-Cancer Drug Des.* **2000**, *15*, 323.
- [18] A. J. Barton, W. Levason, G. Reid, A. J. Ward, *Organometallics* **2001**, *20*, 3644.
- [19] E. D. Clarke, K. H. Goulding, P. Wardman, *Biochem. Pharmacol.* **1982**, *31*, 3237.
- [20] S. M. Evans, C. J. Koch, *Cancer Lett.* **2003**, *195*, 1.
-